LA-UR-17-27729 (Accepted Manuscript)

PT-symmetry in kagome photonic lattices

Chern, Gia-Wei
Saxena, Avadh

To be published in:

DOI to publisher's version: 10.1117/12.2274503

Permalink to record: http://permalink.lanl.gov/object/view?what=info:lanl-repo/lareport/LA-UR-17-27729

$\mathcal{PT}$-symmetry in kagome photonic lattices

Gia-Wei Chern[a] and Avadh Saxena[b]

[a]Department of Physics, University of Virginia, Charlottesville, VA 22904, USA
[b]Theoretical Division and Center for Nonlinear Studies, Los Alamos National Laboratory, Los Alamos, NM 87545, USA

ABSTRACT

Photonic lattices composed of balanced gain and loss waveguides have attracted considerable attention due of their potential applications in optical beam engineering and image processing. These photonic lattices belong to a larger class of intriguing active metamaterials that exhibit the parity-time ($\mathcal{PT}$) symmetry. Kagome lattice is a two-dimensional network of corner-sharing triangles and is often associated with geometrical frustration. In particular, the frustrated coupling between waveguide modes in a kagome array leads to a dispersionless flat band consisting of spatially localized modes. Recently, a $\mathcal{PT}$-symmetric photonics lattice based on the kagome structure has been proposed by placing $\mathcal{PT}$-symmetric dimers at the kagome lattice points. Each dimer corresponds to a pair of strongly coupled waveguides. With balanced arrangement of gain and loss on individual dimers, the system exhibits a $\mathcal{PT}$-symmetric phase for finite gain/loss parameter up to a critical value. Here we discuss the linear and nonlinear optical beam propagations in this novel $\mathcal{PT}$-symmetric kagome system. The linear beam evolution in this complex kagome waveguide array exhibits a novel oscillatory rotation of optical power along the propagation distance. Long-lived local chiral structures originating from the nearly flat bands of the kagome structure are observed when the lattice is subject to a narrow beam excitation. We further show that inclusion of Kerr-type nonlinearity leads to novel optical solitons.

Keywords: $\mathcal{PT}$-symmetry, photonic lattice, kagome, beam dynamics, soliton

1. INTRODUCTION

The concept of parity-time ($\mathcal{PT}$) symmetry has attracted considerable attention in diverse areas of science since the discovery of the fact that a specific class of non-Hermitian Hamiltonians may exhibit entirely real eigenvalue spectra in a certain parameter range.[1,2] A necessary condition for the Hamiltonian to be $\mathcal{PT}$ symmetric is that its complex potential $V(\mathbf{r})$ satisfies the spatial symmetry constraint $V(\mathbf{r}) = V^*(-\mathbf{r})$, i.e. the real part of the complex potential must be an even function of position whereas the imaginary component should be odd. Another important feature of such non-Hermitian Hamiltonians is the phenomenon of spontaneous breaking of the $\mathcal{PT}$-symmetry: the system is in the so-called exact phase with entirely real eigenvalues for a small gain and loss coefficient, and undergoes a transition into a phase with broken $\mathcal{PT}$-symmetry as this gain/loss coefficient increases. Among the various physical implementations, the complex $\mathcal{PT}$-symmetric potentials can be realized in the most straightforward way in optics by combining the spatial modulation of the refractive index with properly balanced gain and loss.[3–5] In particular, $\mathcal{PT}$-symmetric waveguide array,[3] which is equivalent to complex tight-binding system, provides a simple but nontrivial framework for the study of such non-Hermitian Hamiltonian systems.

Motivated by recent experimental developments,[4,5] $\mathcal{PT}$-symmetric photonic lattices have been theoretically studied in various geometries, including the one-dimensional (1D) chain[6,7] and ladder,[8] as well as 2D square,[6] honeycomb,[9,10] and triangular lattices.[11] Several intriguing features have been observed including, among others, power oscillation, double diffraction, and a new type of conical diffraction. Inclusion of nonlinearity also leads to several new soliton solutions.[11–14] Recently, frustrated photonic lattices that exhibit flat bands have generated significant interest among researchers due to their fundamental interest and practical applications. The presence of flat bands indicates a macroscopic degeneracy of the eigenmodes. The superposition of these degenerate modes

Further author information: (Send correspondence to G.-W. C.)
G.-W. C.: E-mail: gchern@virginia.edu

gives rise to highly localized stationary structures even in the absence of nonlinearity. Consequently, diffraction-free transmission can be achieved in such lattices by decomposing a given image into the local modes.[15] The significantly reduced dispersion of the flat band also indicates enhanced nonlinear effects.[16,17] Such localized states have recently been demonstrated experimentally in optical Lieb[18–20] and kagome[21] lattices. In particular, kagome is one of the most extensively studied structure in highly frustrated magnets.[22] In addition to the flat band, the kagome spectrum also contains several topologically nontrivial band-crossing points; gapping out these points could lead to optical topological phases.

Recently, we have proposed a novel kagome photonic lattice that exhibits a $\mathcal{PT}$-symmetric phase;[23] see Fig. 1. Our strategy is to build the complex waveguide array based on $\mathcal{PT}$-symmetric dimers, which have been shown to play an important role in realizing an exact $\mathcal{PT}$-symmetric phase in other structures.[8,13] A $\mathcal{PT}$-symmetric dimer is a pair of strongly coupled waveguides with balanced gain and loss $\pm i\gamma$. In fact, optical lattices built from such dimers possess a local $\mathcal{PT}$ symmetry associated with each dimer and are rather robust against disorder.[8] On the other hand, the dimerization also significantly lowers the lattice symmetry. For example, in order to realize the exact $\mathcal{PT}$ phase, the C_3 symmetry is lost in the complex triangular and honeycomb lattices proposed in Refs. 9–11. Our proposed lattice structure, on the other hand, can be viewed as two interpenetrating twisted kagome lattices. The waveguides with gain form one twisted kagome, while waveguides with loss reside on the other kagome twisted in the opposite direction; see Fig. 1(b). Since the chirality of the two kagome sublattices are opposite to each other, the overall structure not only possesses the $\mathcal{PT}$ symmetry, but also retains the C_3 point group symmetry. We believe this structure is the simplest $\mathcal{PT}$ lattice that also respects the three-fold rotation symmetry. A similar procedure can be used to construct a 2D lattice with both $\mathcal{PT}$ and C_4 symmetries.

Another interesting feature of our system is that the kagome lattice is isostatic mechanically, and twisting corresponds to a mechanical zero mode that preserves the nearest-neighbor bond length. Consequently, the two (twisted) kagome sublattices separately preserve the flat band. Introducing couplings between the two kagome sublattices produces coupled $\mathcal{PT}$-dimers and lifts their individual macroscopic degeneracy. Nonetheless, our calculation shows that the system still exhibits two nearly flat bands in the $\mathcal{PT}$-symmetric phase. We note in passing that the effects of $\mathcal{PT}$-symmetric perturbation to quasi-1D flat-band systems have recently been investigated theoretically.[24,25] These studies show that the quasi-1D flat-band lattices fail to display a $\mathcal{PT}$-symmetric phase with entirely real eigenvalue spectrum once such complex perturbations are introduced. Our proposed kagome structure, on the other hand, exhibits an exact $\mathcal{PT}$-symmetric phase with two nearly flat bands when the gain/loss perturbation is below a threshold value $\gamma < \gamma_c$.

In this paper, we will first discuss the model, bandstructure and the $\mathcal{PT}$-symmetric phase of the kagome dimer lattice in Sec. 2. We shot that the $\mathcal{PT}$-symmetry breaking transition occurs when the two nearly flat bands collapse at the Brillouin zone center. In Sec. 3, we present our linear beam dynamics simulations, which uncover interesting oscillatory rotations of optical power along the propagation distance. In particular, we find long-lived local chiral structures consisting of quasi-local modes when the lattice is subject to a narrow beam excitation. By including Kerr-type focusing nonlinearity, we find stable soliton solutions that are discussed in Sec. 4. These solitons are rather large object consisting of tens of waveguides. Finally, we briefly summarize our results in Sec. 5.

2. BAND STRUCTURE

The complex kagome lattice is depicted in Fig. 1. It consists of $\mathcal{PT}$-symmetric dimers placed at vertices of each triangle of the kagome lattice. Since the kagome-lattice sites correspond to bonds in the dual honeycomb lattice, the same structure can be obtained by placing dimers on the bonds of the honeycomb lattice, with dimer orientations perpendicular to the bonds. Each dimer consists of two types of waveguides: type A is made of gain material, whereas type B exhibits an equal amount of loss. As discussed above, our kagome-dimer structure can also be viewed as two interpenetrating twisted kagome lattices: the A (gain) sublattice itself forms a twisted kagome lattice, while the B (loss) waveguides are arranged in another twisted kagome with opposite chirality. We assume that each waveguide supports only one mode, while light is transferred between neighboring waveguides through optical tunneling. In the tight-binding description,[26] the diffraction dynamics of the optical

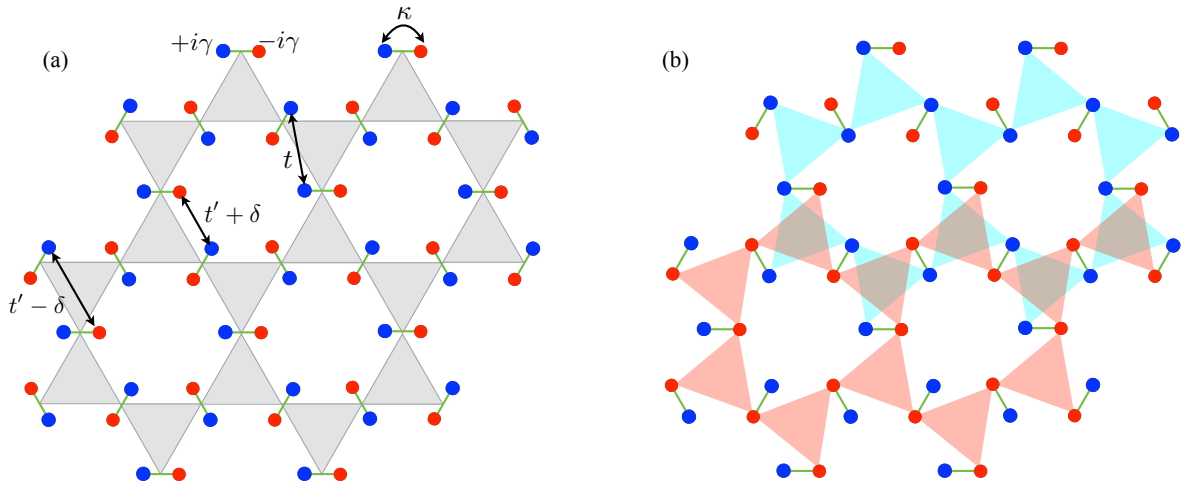

Figure 1. (a) kagome photonic lattice consisting of $\mathcal{PT}$-symmetric dimers. The blue and red circles denote waveguides with a gain and a loss parameter $\pm i\gamma$, respectively. κ is the intra-dimer coupling, while t and $t' \pm \delta$ denote the nearest-neighbor (NN) couplings between same and different sublattices, respectively. (b) The lattice can also be viewed as two interpenetrating twisted kagome lattices. The waveguides with gain (blue) form one twisted kagome sublattice, while waveguides with loss (red) form another twisted kagome with opposite chirality. The combined structure still preserves a C_3 discrete rotation symmetry.

field amplitude $\Psi_n = (a_n, b_n)^T$ at the n-th dimer evolves according to the following coupled-mode equation:

$$
\begin{aligned}
i\frac{da_n}{dz} &= +i\gamma\, a_n + \kappa\, b_n + \sum_m^{\mathrm{NN}} [t\, a_m + (t' \pm \delta)\, b_m] + \chi |a_n|^2\, a_n, \\
i\frac{db_n}{dz} &= -i\gamma\, b_n + \kappa\, a_n + \sum_m^{\mathrm{NN}} [t\, b_m + (t' \pm \delta)\, a_m] + \chi |b_n|^2\, b_n.
\end{aligned} \tag{1}
$$

Here γ is the gain/loss parameter, κ is the dominant intra-dimer coupling, χ is the Kerr-type nonlinear coupling coefficient,[27] t is the nearest-neighbor (NN) coupling constant between waveguides of same sublattices, $t' \pm \delta$ denote the two distinct NN couplings between different sublattices; see Fig. 1. The summation above is restricted to the NN pairs. We first analyze the linear bandstructure of the kagome dimer structure and set $\chi = 0$. To this end, we note that the kagome site index can be represented as $n = (s, \mathbf{r}_n)$, where $s = 1, 2, 3$ indicates the three sublattices of kagome, and $\mathbf{r}_n$ denotes the Bravais lattice point of the underlying triangular lattice. After introducing a Fourier transform for field amplitude $a_n = (1/\sqrt{N}) \sum_{\mathbf{k}} a_{s,\mathbf{k}} \exp(i\mathbf{k}\cdot\mathbf{r}_n)$ and a similar expression for b_n, the coupled-mode equations become

$$
i\frac{d}{dz}\begin{pmatrix} \vec{a}_{\mathbf{k}} \\ \vec{b}_{\mathbf{k}} \end{pmatrix} = \begin{pmatrix} \mathcal{P}_{\mathbf{k}} & \mathcal{Q}_{\mathbf{k}} \\ \mathcal{Q}_{\mathbf{k}}^{\dagger} & \mathcal{P}_{\mathbf{k}}^{\dagger} \end{pmatrix} \begin{pmatrix} \vec{a}_{\mathbf{k}} \\ \vec{b}_{\mathbf{k}} \end{pmatrix} \tag{2}
$$

where $\vec{a}_{\mathbf{k}} = (a_{1,\mathbf{k}}, a_{2,\mathbf{k}}, a_{3,\mathbf{k}})^T$, $\vec{b}_{\mathbf{k}} = (b_{1,\mathbf{k}}, b_{2,\mathbf{k}}, b_{3,\mathbf{k}})^T$, and the two 3×3 matrices $\mathcal{P}$ and $\mathcal{Q}$ are

$$
\mathcal{P}_{\mathbf{k}} = \begin{pmatrix} i\gamma & tc_3 & tc_2 \\ tc_3 & i\gamma & tc_1 \\ tc_2 & tc_1 & i\gamma \end{pmatrix}, \qquad \mathcal{Q}_{\mathbf{k}} = \begin{pmatrix} \kappa & t'c_3 - i\delta s_3 & t'c_2 - i\delta s_2 \\ t'c_3 + i\delta s_3 & \kappa & t'c_1 + i\delta s_1 \\ t'c_2 + i\delta s_2 & t'c_1 - i\delta s_1 & \kappa \end{pmatrix}. \tag{3}
$$

For convenience, we have introduced factors $c_i = 2\cos(\mathbf{k}\cdot\mathbf{d}_i)$ and $s_i = 2\sin(\mathbf{k}\cdot\mathbf{d}_i)$ $(i = 1, 2, 3)$, the three vectors $\mathbf{d}_{1,2} = a(1, \mp\sqrt{3})/4$, $\mathbf{d}_3 = a(1/2, 0)$ connect the neighboring sites on kagome, and a is the lattice constant. The dispersion relations of the eigenmodes are given by the stationary solutions $\Psi_{\mathbf{k}} \sim \exp(i\beta z)$, where the propagation constant $\beta = \beta(\mathbf{k})$ is the eigenvalue of the tight-binding matrix in Eq. (2).

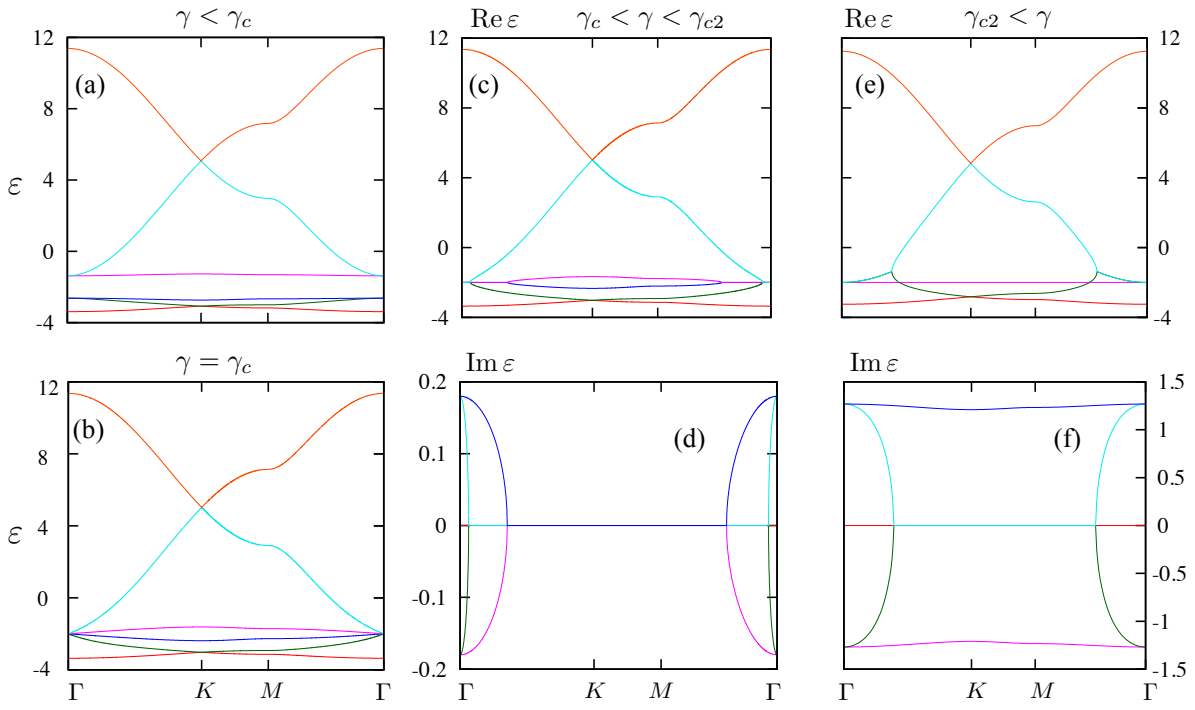

Figure 2. Band structure of the kagome dimer lattice along high-symmetry directions for varying gain and loss parameter γ. The coupling constants (in units of the NN coupling t) are $\kappa = 3$, $t' = 1.1$, and $\delta = 0.1$. The critical $\gamma_c = 0.8$. (a) and (b) show the (completely) real spectra when $\gamma = 0.7$ and $\gamma = \gamma_c$, respectively. (c) and (d) show the real and imaginary parts, respectively, of the eigen-spectrum for $\gamma = 1.2$. (e) and (f) show the real and imaginary parts, respectively, of $\beta(\mathbf{k})$ at even higher $\gamma = 2.0$.

As is well established in other non-Hermitian systems, the $\mathcal{PT}$ symmetry is a necessary but not a sufficient condition for the reality of the eigenvalue spectrum. By using spectral techniques we numerically determined the existence of a $\mathcal{PT}$ threshold γ_c, below which the propagation constants of all bands and wave vectors are real. The critical γ_c depends on coupling constants κ and t', to be discussed below. Above this threshold, the system undergoes a transition into a phase with partially complex eigenvalues β. Fig. 2(a) shows the band structure of the kagome lattice when $\gamma < \gamma_c$. This spectrum inherits several features characteristic of the kagome tight-binding model; it can be viewed as two (scaled) copies of the kagome spectrum. First, there are two pairs of Dirac points located at the corners of the Brillouin zone.[16] Second, there are two quadratic band crossing points at the zone center. These quadratic crossing points are topologically nontrivial in the sense that each of them carries a 2π Berry flux. Finally, there are two nearly flat bands (the 3rd and 4th) due to geometrical frustration; the weak dispersion is caused by the coupling between the two twisted kagome sublattices A and B.

The two nearly flat bands are separated by a finite gap Δ as shown in Fig. 2(a). With increasing gain/loss parameter, the closing of the gap at $\mathbf{k} = 0$ coincides with the $\mathcal{PT}$-symmetry breaking transition. Analytical calculation finds a gap $\Delta_\Gamma = 2\sqrt{(\kappa - 2t')^2 - \gamma^2}$ at the Γ point. Setting $\Delta_\Gamma = 0$ gives the critical value for the $\mathcal{PT}$ transition: $\gamma_c = \kappa - 2t'$, which is independent of t and δ. The two topological quadratic band-crossing points merge at the Brillouin zone center when $\gamma = \gamma_c$; see Fig. 2(b). The $\mathcal{PT}$ phase transition here exhibits all the characteristics of an exceptional-point singularity. Other than the coalescing of eigenmodes, signaling a collapsed Hilbert space, we have also confirmed numerically a divergent Petermann factor[28,29] when $\gamma \to \gamma_c$. In the $\mathcal{PT}$-symmetry breaking phase, the two original nearly flat bands coalesce completely when $\gamma > \gamma_{c2}$. The real part of the coalesced band is doubly degenerate and becomes perfectly flat; its imaginary part is nonzero throughout the whole Brillouin zone.

3. LINEAR BEAM DYNAMICS

The complex guiding potentials also have profound effects on linear beam dynamics of the kagome waveguide arrays. By exciting the $\mathcal{PT}$-symmetric lattice with a Gaussian beam at $z = 0$, we numerically integrate Eq. (1) for a large system with up to 6×10^4 waveguides. We first consider the situation when the array is excited by a wide beam of width $w_0 = 5.5a$; the center of the beam coincides with one of the triangle center. For a passive kagome lattice, the beam evolution follows the standard diffraction pattern as shown in Fig. 3(a). The envelop of the optical field remains circularly symmetric with respect to the beam center, while its amplitude slowly decays with distance. On the other hand, the intensity profile, Fig. 3(b), of a complex array with $\gamma = 0.75$ exhibits a rather inhomogeneous power distribution within individual dimers. As the optical power oscillates in the kagome lattice, the radial profile of $|\Psi|^2$ shows multiple branches. Detailed examination reveals that the optical field rotates periodically about the beam center. To quantify this oscillatory rotation, we first compute the angular Fourier components of the intensity profile: $\mathcal{F}_m \equiv \sum_n |\Psi_n|^2 \exp(im\,\theta_n)$, where m is an integer, and $\theta_n = \arctan(y_n/x_n)$ is the angular coordinate of the nth waveguide. The fact that the optical field maintains a C_3 symmetry indicates that the first nontrivial higher harmonic is $m = 3$. We can then define an angle $\Theta_3 \equiv \arctan[\mathrm{Im}(F_3)/\mathrm{Re}(F_3)]$ to measure the shift of the optical power from the C_3 symmetric axis of the lattice. For a passive lattice, this angle remains zero throughout the beam propagation. On the contrary, Θ_3 oscillates with z in the exact $\mathcal{PT}$-symmetric phase of the kagome lattice; see Fig. 4(a). This result is reminiscent of the power oscillation phenomena of a single $\mathcal{PT}$ dimer.

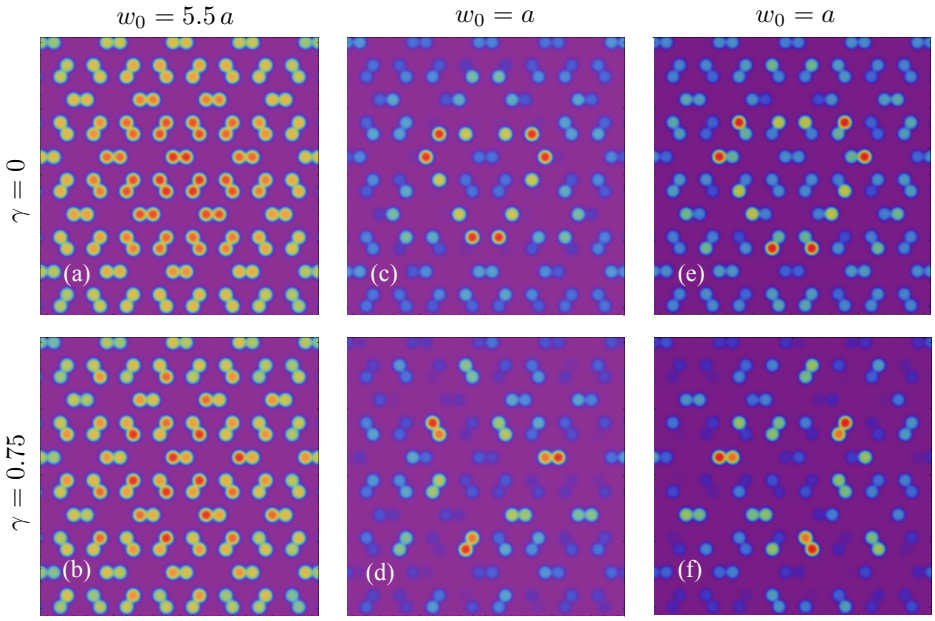

Figure 3. (a) and (b) show snapshots of the intensity profile $|\Psi_n|^2$ under wide beam excitations for (a) a passive array ($\gamma = 0$) and (b) a complex array with $\gamma = 0.75$; the width of the incident beam is $w_0 = 5.5a$. (c)–(f) show snapshots of the quasi-stationary local structure under narrow beam excitations ($w_0 = a$) for (c), (e) a passive array ($\gamma = 0$) and (d), (f) a complex array with $\gamma = 0.75$.

An input beam with a narrow width excites a broad range of eigenmodes including those in the nearly flat bands. After the optical power spreads over the lattice through the dispersive modes, a long-lived local structure remains in the central region of the input beam. These local structures are quasi-stationary. For example, in a passive array, the intensity profile oscillates between the two patterns shown in Fig. 3(c) and (e); the pattern repeats itself with a period $\Delta z \approx 3.5$. The introduction of gain/loss to the waveguides gives rise to a *chiral* local structure; two snapshots of such local patterns are shown in Fig. 3(d) and (f) for a $\mathcal{PT}$-symmetric kagome lattice with $\gamma = 0.78$. The dynamical evolution of the local structures is more complex than that of a passive array. Again, while maintaining a C_3 symmetry, the chiral pattern rotates about the beam axis. This is illustrated in

Fig. 4(b) which shows the angle Θ_3 as a function of propagation distance z for a narrow beam excitation. The chiral nature of the local structure also manifests itself in the beam dynamics: the moving average of Θ_3 deviates significantly from zero especially at large z.

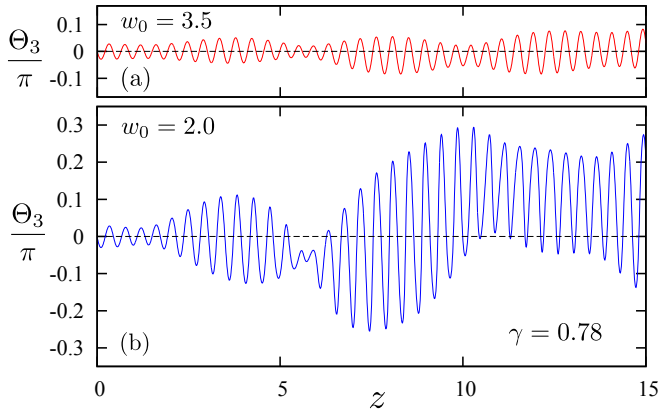

Figure 4. The oscillatory power rotations in a $\mathcal{PT}$-symmetric kagome lattice ($\gamma = 0.78$) for (a) wide and (b) narrow beam excitations.

4. FUNDAMENTAL SOLITONS

In this section, we consider the effect of Kerr-type focusing nonlinearity in the kagome $\mathcal{PT}$-symmetric waveguide arrays. For light propagation in a Kerr-type medium, the refractive index is a function of the field intensity, i.e. $n(\mathbf{r}, |\Psi|^2) = n(\mathbf{r}) + n_2 |\Psi|^2$. The nonlinear coefficient χ in Eq. (1) is proportional to the Kerr coefficient n_2. Inclusion of nonlinearity in the fundamental $\mathcal{PT}$-symmetric dimer leads to intriguing phenomena such as unidirectional propagation of optical waves.[30,31] Localized nonlinear modes or solitons are also shown to exist in both 1D and 2D photonic lattices with $\mathcal{PT}$-symmetry.[11–14] In particular, the exact soliton solution of a $\mathcal{PT}$-symmetric dimer exhibits several prototypical properties of such nonlinear modes in general $\mathcal{PT}$-symmetric systems.[27] First, these soliton solutions form continuous families which can be parameterized by the propagation constant. Moreover, there exists two branches of such nonlinear modes when the gain/loss parameter γ is below the threshold. At the exceptional point $\gamma = \gamma_c$, these two branches coalesce and become unstable above the $\mathcal{PT}$-symmetry breaking transition. On the other hand, stable soliton solutions have also been examined in kagome systems *without* $\mathcal{PT}$-symmetry.[16,32,33] Our system provides the first realization of optical solitons in a kagome-based structure with $\mathcal{PT}$-symmetry.

To obtain the stationary soliton solution, we search for solutions in the form of $\Psi_n(z) = (a_n, b_n)^T \exp(i\mu z)$, where μ is a real propagation constant. After substituting this ansatz into Eq. (1), we arrive at the following nonlinear eigenvalue equation

$$\begin{aligned} +i\gamma\, a_n + \kappa\, b_n + \sum_m^{\mathrm{NN}} [t\, a_m + (t' \pm \delta)\, b_m] + \chi |a_n|^2\, a_n &= -\mu a_n, \\ -i\gamma\, b_n + \kappa\, a_n + \sum_m^{\mathrm{NN}} [t\, b_m + (t' \pm \delta)\, a_m] + \chi |b_n|^2\, b_n &= -\mu b_n. \end{aligned} \tag{4}$$

Soliton solutions are then obtained using the imaginary-time relaxation method.[34–36] The power of the soliton is defined as $P = \sum_n |\Psi_n|^2$. The imaginary part of the $\mathcal{PT}$-symmetric potential induces inhomogeneous loss, which can generate a lateral gradient force, resulting in the transverse power flow. This local power-flux is given by the Poynting vector of the optical field. In the coupled-mode or tight-binding formulation, the lateral power flux is proportional to the imaginary part of the mode coupling, i.e. $S \propto i\kappa(a_n^* b_n - a_n b_n^*)$,

For γ below the threshold $\gamma_c = \kappa - 2t'$, we numerically construct a family of soliton solutions with real eigenvalues located within the semi-infinite "energy" gap of the linear spectrum. A typical profile of the soliton

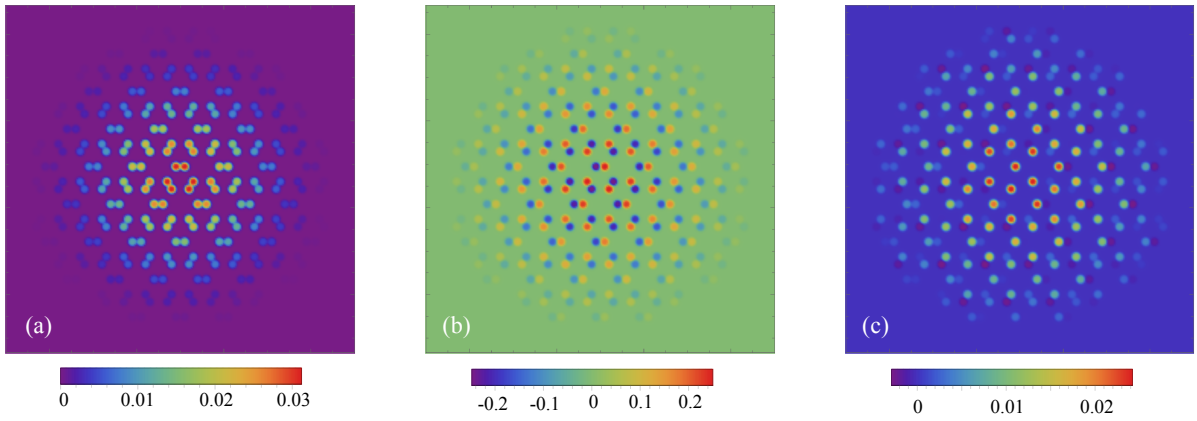

Figure 5. The fundamental soliton of the kagome dimer lattice in the $\mathcal{PT}$-symmetric phase. (a) the intensity profile $I(\mathbf{r}) = |\Psi_n|^2$, (b) the real $\mathrm{Re}\Psi_n$ and (c) imaginary $\mathrm{Im}\Psi_n$ parts of the optical field.

is shown in Fig. 5. The intensity $I(\mathbf{r}) = |\Psi_n|^2$ is well approximated by a Gaussian envelop with a radius of $R \approx 5$ lattice constants. We have also analyzed the stability of the solitons using the standard linearization procedure by adding a small perturbation to the stationary solution. Explicitly, we consider a optical field of the form $\Psi_n = (\Phi_n + F_n e^{i\sigma z} + G_n^* e^{-i\sigma^* z})e^{i\mu z}$, where Φ_n and μ are obtained from the nonlinear stationary equation (4), F_n and G_n are small perturbations. The stability of the nonlinear mode is then determined by the eigenvalue σ of the linearized equation. The growth rate of the instability is then determined by the imaginary part of σ. Similar to previous analysis on solitons in bipartite $\mathcal{PT}$-symmetric lattice, we find that the instability growth rate tends to increase with the gain/loss parameter γ. The real and imaginary parts of the soliton solution are shown in Fig. 5(b) and (c), respectively. It is worth noting that the nontrivial relative phase of Ψ_n at different lattice points indicates a lateral power flow, as discussed above. In general, the direction of the flow is from gain to loss regions. The unbroken C_3 symmetry of the fundamental soliton thus gives rise to an interesting circular pattern of the lateral power flow.

5. CONCLUSION

To summarize, we have presented a kagome based photonic lattice with $\mathcal{PT}$-symmetry and studied its linear beam dynamics and nonlinear optical soliton solutions. The complex waveguide array supports an exact $\mathcal{PT}$-symmetric phase for gain/loss parameter below a finite threshold. The eigen-spectrum in this phase contains two nearly flat bands inherent from the underlying kagome structure. The proposed complex lattice possessing a full C_3 symmetry can be derived from placing $\mathcal{PT}$-symmetric dimers at either the kagome sites or the honeycomb edges. We have uncovered oscillatory power rotation and long-lived chiral local structures in the beam dynamics of the complex kagome lattice. With the inclusion of Kerr-type focusing nonlinearity, we have also obtained a new class of nonlinear self-trapped modes residing in the $\mathcal{PT}$-symmetric kagome photonic lattice.

REFERENCES

[1] C. M. Bender and S. Boettcher, "Real Spectra in Non-Hermitian Hamiltonians Having $\mathcal{PT}$ Symmetry," *Phys. Rev. Lett.* **80**, 5243 (1998).

[2] C. M. Bender, "Making sense of non-Hermitian Hamiltonians," *Rep. Prog. Phys.* **70**, 947 (2007).

[3] R. El-Ganainy, K. G. Makris, D. N. Christodoulides, and Z. H. Musslimani, "Theory of coupled optical PT-symmetric structures," *Opt. Lett.* **32**, 2632 (2007).

[4] A. Guo, G. J. Salamo, D. Duchesne, R. Morandotti, M. Volatier-Ravat, V. Aimez, G. A. Siviloglou, and D. N. Christodoulides, "Observation of $\mathcal{PT}$-Symmetry Breaking in Complex Optical Potentials," *Phys. Rev. Lett.* **103**, 093902 (2009).

[5] C. E. Rüter, K. G. Makris, R. El-Ganainy, D. N. Christodoulides, M. Segev, and D. Kip, "Observation of parity?time symmetry in optics," *Nat. Phys.* **6**, 192 (2010).

[6] K. G. Makris, R. El-Ganainy, D. N. Christodoulides, Z. H. Musslimani, "Beam Dynamics in $\mathcal{PT}$ Symmetric Optical Lattices," *Phys. Rev. Lett.* **100**, 103904 (2008).

[7] S. Longhi, "Bloch Oscillations in Complex Crystals with $\mathcal{PT}$ Symmetry," *Phys. Rev. Lett.* **103**, 123601 (2009).

[8] O. Bendix, R. Fleischmann, T. Kottos, and B. Shapiro, "Optical structures with local $\mathcal{PT}$-symmetry," *J. Phys. A* **43**, 265305 (2010).

[9] A. Szameit, M. C. Rechtsman, O. Bahat-Treidel, and M. Segev, "$\mathcal{PT}$-symmetry in honeycomb photonic lattices," *Phys. Rev. A* **84**, 021806 (2011).

[10] H. Ramezani, T. Kottos, V. Kovanis, and D. N. Christodoulides, "Exceptional-point dynamics in photonic honeycomb lattices with $\mathcal{PT}$ symmetry," *Phys. Rev. A* **85**, 013818 (2012).

[11] H. Wang, S. Shi, X. Ren, X. Zhu, B. A. Malomed, D. Mihalache, Y. He, "Two-dimensional solitons in triangular photonic lattices with parity-time symmetry," *Opt. Commun.* **335**, 146 (2015).

[12] Z. H. Musslimani, K. G. Makris, R. El-Ganainy, and D. N. Christodoulides, "Optical Solitons in $\mathcal{PT}$ Periodic Potentials," *Phys. Rev. Lett.* **100**, 030402 (2008).

[13] S. V. Dmitriev, A. A. Sukhorukov, and Y. S. Kivshar, "Binary parity-time-symmetric nonlinear lattices with balanced gain and loss," *Opt. Lett.* **35**, 2976 (2010).

[14] J. Zeng and Y. Lan, "Two-dimensional solitons in PT linear lattice potentials," *Phys. Rev. E* **85**, 047601 (2012).

[15] R. A. Vicencio and C. Mejia-Cortes, "Diffraction-free image transmission in kagome photonic lattices," *J. Opt.* **16** 015706 (2014).

[16] R. A. Vicencio and M. Johansson, "Discrete flat-band solitons in the kagome lattice," *Phys. Rev. A* **87**, 061803 (2013).

[17] K. J. H. Law, A. Saxena, P. G. Kevrekidis, and A. R. Bishop, "Localized structures in kagome lattices," *Phys. Rev. A* **79** 053818 (2009).

[18] R. A. Vicencio, C. Cantillano, L. Morales-Inostroza, B. Real, C. Mejía-Cortés, S. Weimann, A. Szameit, and M. I. Molina, "Observation of Localized States in Lieb Photonic Lattices," *Phys. Rev. Lett.* **114**, 245503 (2015).

[19] S. Mukherjee, A. Spracklen, D. Choudhury, N. Goldman, P. Öhberg, E. Andersson, and R. R. Thomson, "Observation of a Localized Flat-Band State in a Photonic Lieb Lattice," *Phys. Rev. Lett.* **114**, 245504 (2015).

[20] S. Mukherjee and R. R. Thomson, "Observation of localized flat-band modes in a quasi-one-dimensional photonic rhombic lattice," *Opt. Lett.* **40**, 5443 (2015).

[21] Y. Zong, S. Xia, L. Tang, D. Song, Y. Hu, Y. Pei, J. Su, Y. Li, and Z. Chen, "Observation of localized flat-band states in Kagome photonic lattices," *Opt. Express* **24**, 8877 (2016).

[22] For a review, see P. Mendels and A. S. Wills, Chapter 9 in *Introduction to Frustrated Magnetism*, ed. C. Lacroix, P. Mendels, and F. Mila (Springer Verlag, Berlin 2011).

[23] G.-W. Chern and A. Saxena, "$\mathcal{PT}$-symmetric phase in kagome photonic lattices," *Opt. Lett.* **40**, 5806 (2015).

[24] L. Ge, "Parity-time symmetry in a flat-band system," *Phys. Rev. A* **92**, 052103 (2015).

[25] M. I. Molina, "Flat bands and $\mathcal{PT}$ symmetry in quasi-one-dimensional lattices," *Phys. Rev. A* **92**, 063813 (2015).

[26] Y. N. Joglekar, C. Thompson, D. D. Scott, and G. Vemuri, "Optical waveguide arrays: quantum effects and PT symmetry breaking," *Eur. Phys. J. Appl. Phys.* **63**, 30001 (2013).

[27] V. V. Konotop, J. Yang, and D. A. Zezyulin, "Nonlinear waves in $\mathcal{PT}$-symmetric systems," *Rev. Mod. Phys.* **88**, 035002 (2016).

[28] M. C. Zheng, D. N. Christodoulides, R. Fleischmann, and T. Kottos, "$\mathcal{PT}$-optical lattices and universality in beam dynamics," *Phys. Rev. A* **82**, 010103 (2010).

[29] K. Petermann, "Calculated spontaneous emission factor for double-heterostructure injection lasers with gain-induced waveguiding," *IEEE J. Quantum Electron.* **15**, 566 (1979).

[30] H. Ramezani, T. Kottos, R. El-Ganainy, and D. N. Christodoulides, "Unidirectional nonlinear $\mathcal{PT}$-symmetric optical structures," *Phys. Rev. A* **82**, 043803 (2010).

[31] A. A. Sukhorukov, Z. Xu, and Y. S. Kivshar, "Nonlinear suppression of time reversals in $\mathcal{PT}$-symmetric optical couplers", *Phys. Rev. A* **82**, 043818 (2010).

[32] X. Zhu, H. Wang, L.-X. Zheng, "Defect solitons in kagome optical lattices," *Opt. Express* **18**, 20786 (2010).

[33] M. I. Molina, "Localized modes in nonlinear photonic kagome nanoribbons", *Phys. Lett. A* **376**, 3458 (2012).

[34] J. Yang and T. I. Lakoba, "Accelerated Imaginary-time Evolution Methods for the Computation of Solitary Waves," *Stud. Appl. Math.* **120**, 265 (2008).

[35] M. L. Chiofalo, S. Succi, and M. P. Tosi, "Ground state of trapped interacting Bose-Einstein condensates by an explicit imaginary-time algorithm," *Phys. Rev. E* **62**, 7438 (2000).

[36] L. D. Carr and Y. Castin, "Dynamics of matter-wave bright soliton in an expulsive potential," *Phys. Rev. A* **66**, 063602 (2002).